Geophysical Research Letters

RESEARCH LETTER
10.1029/2024GL112368

The Cloud Radiative Response to Surface Warming Weakens Hydrological Sensitivity

Zachary McGraw[1,2], Lorenzo M. Polvani[1,3,4], Blaž Gasparini[5], Emily K. Van de Koot[6], and Aiko Voigt[5]

[1]Department of Applied Physics and Applied Mathematics, Columbia University, New York, NY, USA, [2]NASA Goddard Institute for Space Studies, New York, NY, USA, [3]Department of Earth and Environmental Sciences, Columbia University, New York, NY, USA, [4]Lamont-Doherty Earth Observatory, Columbia University, Palisades, NY, USA, [5]Department of Meteorology and Geophysics, University of Vienna, Vienna, Austria, [6]Atmospheric, Oceanic and Planetary Physics, University of Oxford, Oxford, UK

Key Points:

- Cloud radiative responses to surface warming weaken the global mean precipitation increase per degree of warming
- High clouds are a prominent source of intermodel disagreement for the atmosphere's radiative and precipitation responses to surface warming
- Cloud locking experiments enable quantification and detailed study of how cloud radiative responses to warming affect precipitation change

Supporting Information:

Supporting Information may be found in the online version of this article.

Correspondence to:

Z. McGraw,
zachary.mcgraw@columbia.edu

Citation:

McGraw, Z., Polvani, L. M., Gasparini, B., Van de Koot, E. K., & Voigt, A. (2025). The Cloud radiative response to surface warming weakens hydrological sensitivity. *Geophysical Research Letters*, *52*, e2024GL112368. https://doi.org/10.1029/2024GL112368

Received 3 SEP 2024
Accepted 24 NOV 2024

Author Contributions:

Conceptualization: Zachary McGraw, Lorenzo M. Polvani
Data curation: Blaž Gasparini, Emily K. Van de Koot, Aiko Voigt
Formal analysis: Zachary McGraw
Funding acquisition: Lorenzo M. Polvani
Investigation: Zachary McGraw
Methodology: Zachary McGraw, Lorenzo M. Polvani
Resources: Blaž Gasparini, Emily K. Van de Koot, Aiko Voigt
Supervision: Lorenzo M. Polvani
Visualization: Zachary McGraw
Writing – original draft: Zachary McGraw

Abstract Precipitation is expected to increase in a warmer global climate, yet how sensitive precipitation is to warming depends on poorly constrained cloud radiative processes. Clouds respond to surface warming in ways that alter the atmosphere's ability to radiatively cool and hence form precipitation. Here we examine the links between cloud responses to warming, atmospheric radiative fluxes, and hydrological sensitivity in AMIP6 simulations. The clearest impacts come from high clouds, which reduce atmospheric radiative cooling as they rise in altitude in response to surface warming. Using cloud locking, we demonstrate that high cloud radiative changes weaken Earth's hydrological sensitivity to surface warming. The total impact of cloud radiative effects on hydrological sensitivity is halved by interactions between cloud and clear-sky radiative effects, yet is sufficiently large to be a major source of uncertainty in hydrological sensitivity.

Plain Language Summary Clouds both absorb and emit radiation, with the net balance influencing how readily precipitation can form in the atmosphere. Here we look at how clouds alter the atmosphere's radiative response to warming and through this affect how much precipitation will increase in a warmer climate. We find that high clouds, which are known to rise as the surface warms, drive considerable disagreement in simulated radiative and precipitation responses to warming. By analyzing simulations where the radiative influences of clouds are locked into place, we demonstrate that these influences overall reduce the precipitation increase per degree of warming. Our analysis also reveals complicating factors affecting the link between cloud and precipitation changes in a warmer climate.

1. Introduction

Cloud responses to warming are one of the main uncertainties for projections of future climate (Sherwood et al., 2020; Zelinka et al., 2020). While extensive research has examined how cloud responses alter the extent of global greenhouse gas warming, the question of how these cloud responses affect future precipitation remains largely unexplored. Surface temperature is governed by Earth's top-of-atmosphere (TOA) radiative balance, while precipitation is more directly controlled by radiative fluxes into and out of the atmosphere, from Earth's surface as well as space. In the atmospheric (ATM) energy budget, radiative cooling drives the cycling of latent heat into the atmosphere by condensation, with surface precipitation rates reflecting the net release of latent heat. As clouds are a major term in both the TOA and ATM energy budgets, some of the cloud radiative responses to surface warming that amplify or dampen this warming (i.e., *cloud feedbacks*) will also affect how strongly precipitation responds to surface warming (*hydrological sensitivity* or HS). Here we use recently available methods to establish how cloud radiative processes influence the atmosphere's energetic and hydrological responses.

Over spatial scales of several thousand kilometers or more, any changes in latent heat from precipitation ($L\Delta P$, where L is the latent heat of condensation and P is surface precipitation averaged over months or years) must be balanced by changes in atmospheric radiative cooling ($-\Delta R_{ATM}$) plus changes in surface-to-atmosphere sensible heat flux (ΔSH) (Muller & O'Gorman, 2011; O'Gorman et al., 2012). The atmospheric energy budget is hence a useful framework for understanding precipitation change, despite not directly revealing cause-and-effect relationships on its own. Atmospheric radiative flux changes can be decomposed into a clear-sky component that is calculated by ignoring clouds in calculations of radiative energy fluxes (ΔR_{clear}) and cloud radiative effects

Writing – review & editing: Zachary McGraw, Lorenzo M. Polvani, Blaž Gasparini, Emily K. Van de Koot, Aiko Voigt

(ΔCRE), which are calculated as the difference between the full and clear-sky fluxes. Defining all positive fluxes to add energy into the atmosphere, this relationship can be written as

$$L\Delta P = -\Delta R_{ATM} - \Delta SH = -\Delta CRE - \Delta R_{clear} - \Delta SH \quad (1)$$

The clear-sky radiative change is the net result of tropospheric temperature and water vapor concentration both increasing as the surface warms. For warming within several degrees of present-day global climate, clear-sky radiative responses overall increase both atmospheric radiative cooling and precipitation (Jeevanjee & Romps, 2018; Liu et al., 2024). Despite this clear-sky basis, much of the intermodel spread in HS has been shown to be associated with cloud radiative responses (Previdi, 2010). Low and high clouds have opposite roles in the present atmosphere's ability to radiatively cool, tending toward net radiative cooling and heating, respectively (Voigt, North, et al., 2024). Past efforts to link cloud radiative effects to HS have relied on correlations among models through the *emergent constraint* framework, with the predominant focus being on low clouds (e.g., Hendrickson et al., 2021; Watanabe et al., 2018; Zhou et al., 2023). However, there is limited confidence in these relationships, as shown by Pendergrass (2020).

Here we carefully examine the atmospheric radiative impacts of cloud responses to surface warming in several climate models. We then link these responses to HS, focusing on the percent precipitation increase per Kelvin of surface warming without factoring in rapid adjustments to CO_2 or other potential causes of the warming. Our analysis brings to this effort three recently available tools: (a) vertically resolved radiative flux responses to warming, (b) cloud radiative kernels for radiative fluxes within the atmosphere, (c) and the cloud locking method. With these tools, we will reveal that high cloud radiative responses to warming considerably alter the Earth's atmospheric energy budget and through this influence HS.

2. Methods

2.1. AMIP6 Climate Model Simulations

We base the majority of our analysis on Atmospheric Model Intercomparison Project Phase 6 (AMIP6; Eyring et al., 2016) simulations, wherein sea surface temperatures (SSTs) are prescribed to the same values in all models rather than calculated with coupled ocean models. For each model, we evaluate surface warming impacts by comparing simulations with SSTs over the years 1979–2014 to equivalent simulations with 4 K warming uniformly applied globally. We averaged all simulations across these years after confirming that 1979 model output did not indicate a problematic spin-up year. For our analysis, we use 11 models having detailed outputs directed by the Cloud Feedback Model Intercomparison Project (CFMIP). This includes all models with the satellite simulator output needed for the cloud kernel analysis described below, although we limit our analysis to one ensemble member per modeling center, choosing each center's first numbered simulation.

To calculate the convergence or divergence of radiative fluxes (i.e., radiative *heating* or *cooling*, respectively), we use vertically resolved radiative fluxes that are available for 7 of the 11 models. We follow the method detailed in Voigt, North, et al. (2024) to calculate cloud radiative heating (CRH), and likewise calculate clear-sky radiative heating (which is typically negative, i.e. net cooling). By integrating the convergences across pressure levels, we calculate cloud and clear-sky radiative effects in both the lower and upper troposphere, which we separate at 680 hPa. We refer to clouds below 680 hPa as *low clouds*, as is standard, and all clouds above this level as *high clouds*. Note that this diverges from previous studies in which clouds above 680 hPa were divided into mid-level and high clouds, with their sum instead referred to as *non-low* clouds (e.g., Zelinka et al., 2016). For the cloud radiative kernel analysis described below, the 680 hPa division corresponds to the pressure of cloud tops, while our analysis of the vertically resolved fluxes separates all cloud layers above and below 680 hPa due to a lack of useable cloud top information here. This separation is meant to approximately distinguish boundary layer and free tropospheric phenomena, which respond differently to a warmer surface.

2.2. Cloud Radiative Kernels

To decompose the mechanisms by which cloud responses to warming drive atmospheric radiative changes, we use the kernel method established by Zelinka et al. (2012a). The AMIP6 models we use were paired to an interactive satellite simulator based on the International Satellite Cloud Climatology Project (ISCCP), as requested by the CFMIP protocol. This simulator records cloud occurrence binned by cloud top pressure and

optical depth in each participating model, while the kernels approximate the radiative impact of a unit change to the cloud occurrence in each bin. Calculations described in Zelinka et al. (2012b) enable the ISCCP output and kernels to be used to estimate radiative impacts of changes in cloud top altitude, cloud amount, and cloud optical depth.

For our calculations, we use the cloud radiative kernels developed by Zhang et al. (2021) based on radiation code from the NASA GISS ModelE2.1 climate model. What makes these kernels particularly useful for our analysis is that they include, for the first time, radiative impacts on the atmospheric energy budget rather than only impacts at top-of-atmosphere. These kernels have previously been applied to AMIP6 data in Y. Zhang, Jin, and Ottaviani (2023), which we here build on by decomposing mechanisms of cloud radiative impacts and relating results to hydrological sensitivity.

2.3. Cloud Locking Experiment

To establish the causal link between cloud radiative changes and their impacts on hydrological sensitivity, we examine a *cloud locking* experiment performed with one model, the Icosahedral Nonhydrostatic (ICON) Modeling Framework (ICON) version 2.6.2.2 (Giorgetta et al., 2018). This experiment was developed for Huber (2024), with simulations described therein, and follows the AMIP protocol (Section 3.1) with additions to isolate impacts of cloud radiative effect changes. In the cloud locking protocol (Voigt & Shaw, 2015), free running simulations are carried out with control SSTs (*T1*) and with SSTs uniformly warmed by 4 K (*T2*). Following this, additional simulations are carried out wherein cloud properties fed into the model's radiation code are "locked" into their states from the free running simulations. This includes simulations where cloud radiative effects are kept in line with the SSTs (simulations *T1C1* and *T2C2*), as well as out-of-sync simulations: one pairing cloud radiative effects from the control to uniformly warmed SSTs (*T2C1*), and one with the opposite combination (*T1C2*). These simulations also have radiative effects of specific humidity locked to values from free running simulations, but as this is outside our focus we did not mismatch SST and humidity states. Slightly simplifying the method in Voigt and Shaw (2015) on this basis, we calculate the effect of cloud radiative responses to surface warming on a variable X as

$$X_{CRE} = ½[(X_{T1C2} - X_{T1C1}) + (X_{T2C2} - X_{T2C1})] \tag{2a}$$

This calculates the cloud effect in each state T1 and T2 and averages the result together without factoring in non-CRE effects. Conversely, the effect of the SST change independent of the cloud effect is calculated as

$$X_{SST} = ½[(X_{T2C1} - X_{T1C1}) + (X_{T2C2} - X_{T1C2})] \tag{2b}$$

3. Results

3.1. Cloud Radiative Impacts on Atmospheric Cooling Response and Its Intermodel Spread

We begin by examining the atmospheric radiative response to surface warming in AMIP6, shown in Figure 1a. The cloud radiative response (red markers) increases the net radiation absorbed by the atmosphere, in opposition to the enhanced clear-sky radiative cooling (gray markers). While the clear-sky response is dominant on average, the cloud radiative response shows a slightly larger intermodel spread globally (panel i) and dominates the spread across the tropics (panel ii, defined throughout this study as 30°S to 30°N). Using vertically resolved output to separate contributions of a lower and upper troposphere split at 680 hPa reveals that the intermodel spread is dominated by high clouds, even though ensemble mean low and high cloud responses are comparable.

Since the free troposphere is expected to expand upward in a warmer climate such that many of its characteristic features stay at similar isotherms (Hartmann & Larson, 2002; Yoshimori et al., 2020), it is sensible to look at the atmosphere's radiative convergence (i.e., heating) along isotherms. We hence interpolated the radiative flux convergences in each control simulation onto isothermal vertical coordinates as in Jeevanjee and Romps (2018). In Figure 1b we show that CRH (panel i) responds very differently across models, dominating the spread in the tropical free troposphere compared to clear-sky responses (panel ii). This is especially clear in the vicinity of 240 K (black horizontal whiskers).

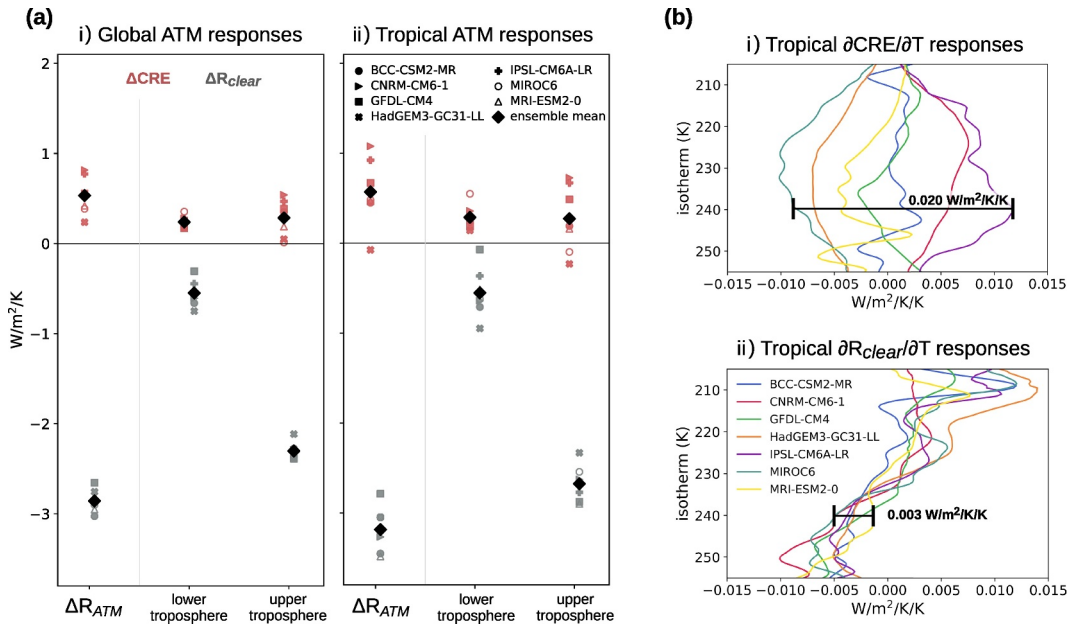

Figure 1. Atmospheric radiative responses to surface warming across AMIP6 models. Shown are radiative responses in the full atmosphere, lower troposphere, and upper troposphere for both cloud and clear-sky fluxes net into the atmosphere (a), and a comparison along free tropospheric isotherms (b).

For a more in depth look at the intermodel spread, we show in Figure 2 the CRH response in each model across latitudes and pressure levels, as in Voigt, North, et al. (2024). At first glance, the upper tropospheric responses (upper row) look qualitatively similar across models, with an arc of enhanced CRH in the upper troposphere and little or opposite impacts in the mid-troposphere. The similar pattern reflects that, in every model, the CRH profile approximately rises to maintain the same isotherms. To demonstrate this we calculate the expected response if the vertical profile of CRH in each model's control simulation simply rose accordingly. We do this by remapping each value in the control simulation to the pressure aloft where temperature is lower by the amount of the underlying surface temperature perturbation (4 K over oceans, with slight deviations over land). As in Po-Chedley et al. (2019), we applied this method only to layers above 600 hPa, as the cloud altitude change applies specifically to the free troposphere. The resulting *predicted* response, shown in the middle row of Figure 2, is qualitatively similar to the actual response in the top row.

However, subtracting the actual and predicted ΔCRH values reveals a sizable remainder that in most models generates radiative heating (bottom row). This results in the positive but poorly constrained upper troposphere values in Figure 1a, which Voigt, North, et al. (2024) had showed in isothermal coordinates. We now look into why high cloud CRH changes with warming, rather than simply being redistributed, and dissimilarly across models.

3.2. Kernel-Derived Radiative Impacts of Cloud Responses to Warming

We next decompose the cloud radiative responses across AMIP6 into their mechanistic causes using the radiative kernels from Zhang et al. (2021), as described in Section 2.2. Figure 3 shows the resulting cloud radiative responses driven by changes in cloud altitude, amount, and optical depth. Kernel estimates agree with the model radiative output (Figure 1a) in establishing that high clouds cause the large spread in the cloud radiative response to warming. Here we now see that all three evaluated mechanisms promote considerable intermodel spread.

Among the quantified mechanisms, the high cloud altitude response is the most robust signal, tending toward enhanced global mean radiative heating in all 11 assessed models (10 of 11 in the tropics). This follows from high clouds rising with warming to altitudes where their temperatures make them less emissive compared to the hypothetical case where high clouds remain at the same altitudes. Though clouds at fixed temperature maintain similar emission to space, these clouds nevertheless radiatively heat as the warmer surface emits enhanced

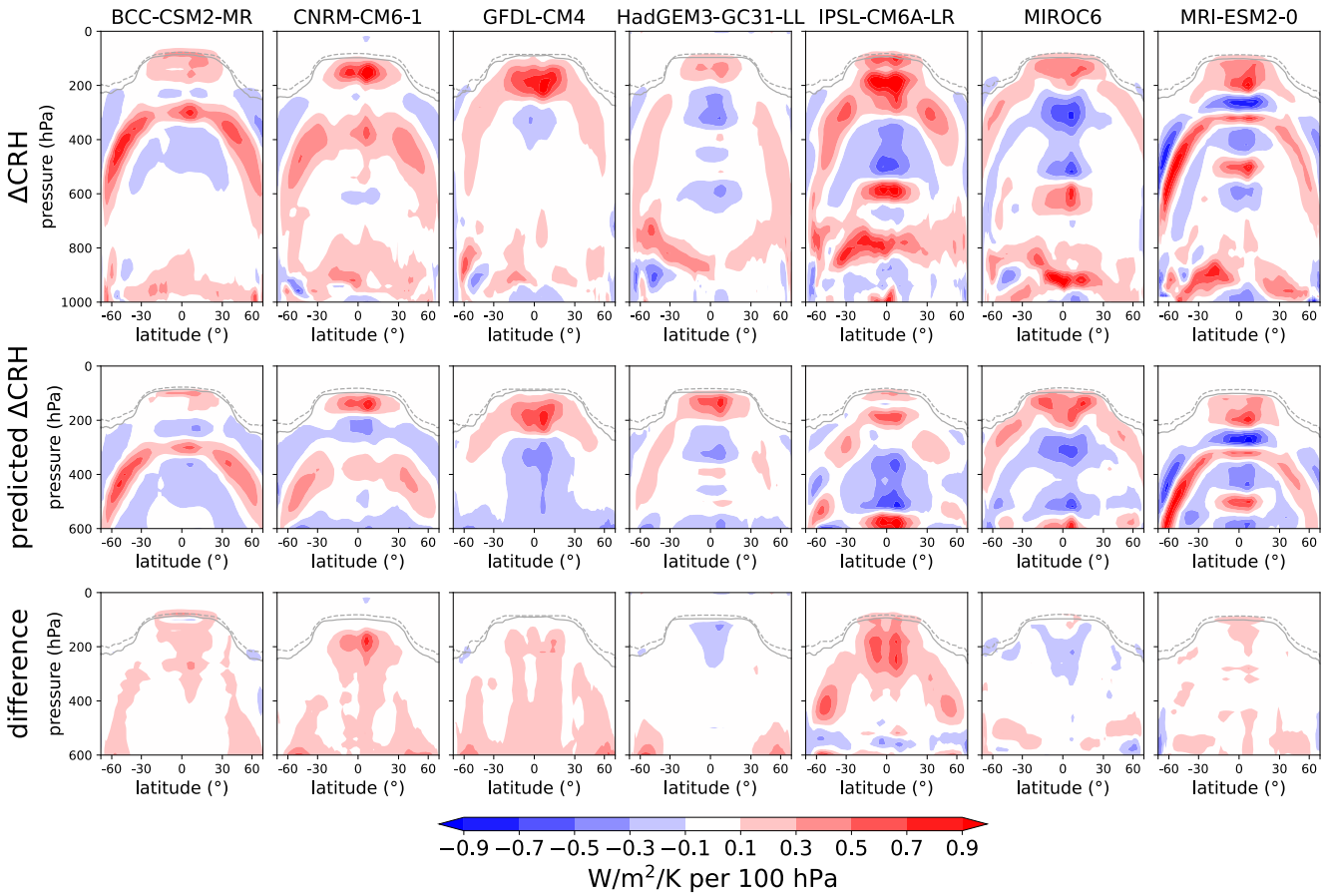

Figure 2. Cloud radiative responses in AMIP6 models compared to the responses that would occur if each cloud radiative heating profile in the control simulation simply rose to be at the same isotherms. Note that for the second and third rows we only show above 600 hPa. Gray solid and dashed lines denote the tropopause in the control and uniformly warmed simulations, respectively.

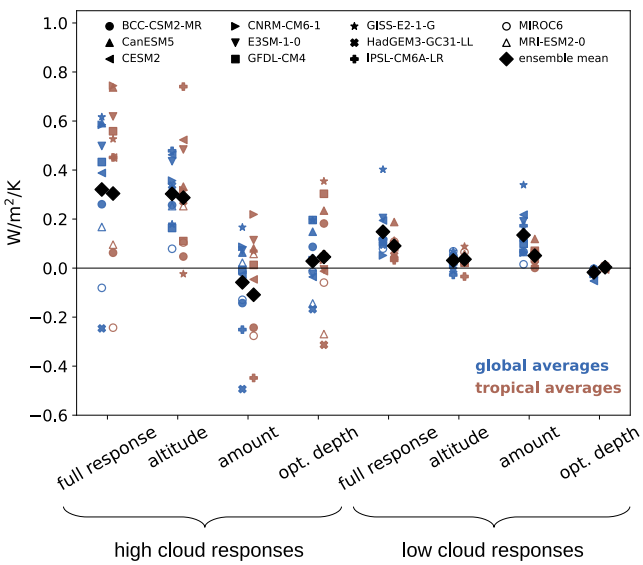

Figure 3. Impacts of cloud responses to surface warming on the atmosphere's radiative balance across AMIP6 models, decomposed with radiative kernels. Results are shown for both global (blue) and tropical (brown) spatial averages.

upward radiative flux that is absorbed by high clouds. The rise in cloud altitude hence increases radiative heating rather than simply shifting it to high altitudes, as seen by the mostly positive differences in the bottom row of Figure 2. In Section 3.4, we will verify that high cloud responses indeed cause enhanced radiative heating as warming occurs. High cloud amount and optical depth responses also greatly contribute to intermodel spread in the cloud radiative response to warming, though both of these responses lack a robust sign across models. On average, however, the amount response slightly counters the altitude response, since high clouds—which overall cause radiative heating—are expected to occupy less volume at higher altitudes (Bony et al., 2016).

We find that the low cloud amount response to warming reduces ATM radiative cooling (see Figure 3), consistent with less cloud that effectively emits longwave emission to the surface. This was postulated by Watanabe et al. (2018), though we find this is not a strong effect, and that it is instead high clouds that dominate AMIP6 intermodel spread in the ATM radiative response to warming. We note separately that the atmospheric radiative response to warming does not directly depend on shortwave responses to nearly the degree as the TOA response (see Figure S1 in Supporting Information S1). Pendergrass and Hartmann (2014) called this "fortuitous" for attempts to constrain HS, as cloud shortwave responses—especially in low

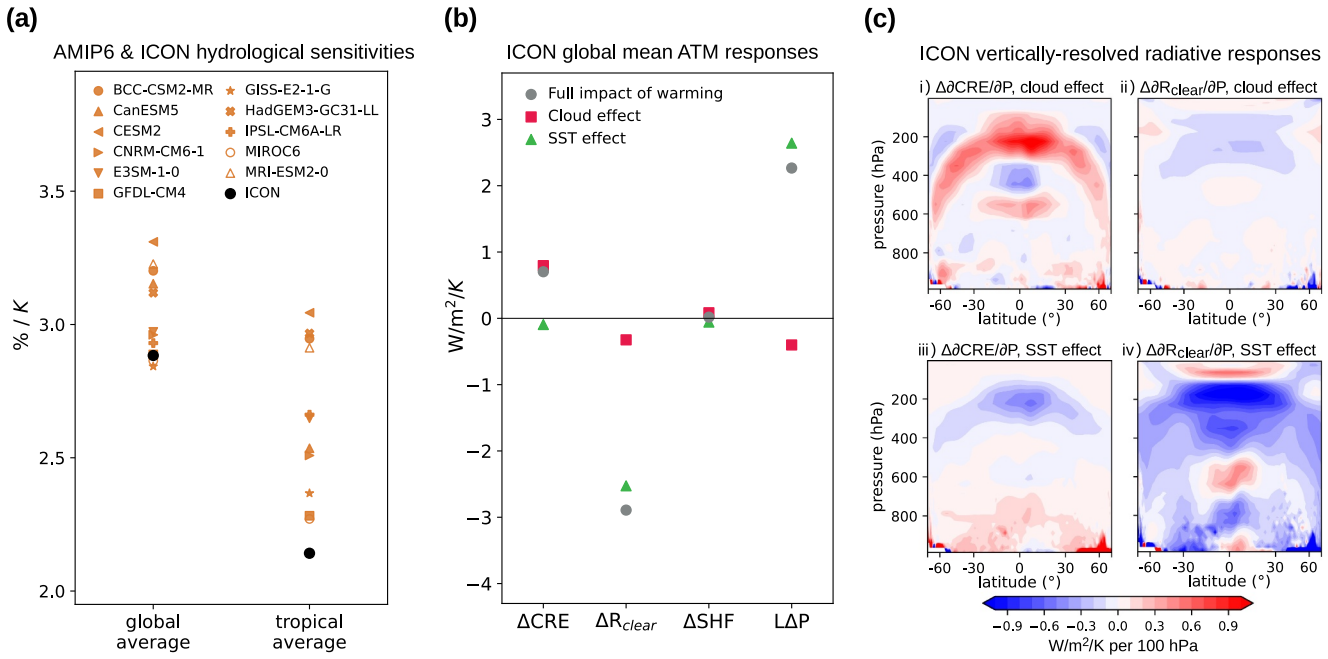

Figure 4. Hydrological sensitivity in AMIP6 experiments and ICON (a) and an in depth look at the influence of cloud radiative responses to warming in an ICON cloud locking experiment (b, c). Cloud and sea surface temperature effects in panels (b, c) were calculated as in Equation 2, while ICON results in panel (a) and the full impacts of warming in panel (b) are from the free-running simulations.

clouds—are extremely uncertain. However, we have shown that longwave high cloud responses are themselves poorly constrained.

3.3. Cloud Radiative Impacts on Hydrological Sensitivity in AMIP6

We now infer hydrological sensitivities from the cloud radiative responses to surface warming we have just described. For the 11 AMIP6 models we have examined, the hydrological sensitivities—defined as the change in precipitation per degree of warming—are shown in Figure 4a (orange markers). While the spread in global average HS is a moderate 2.8%–3.3%/K, the spread in tropical mean HS is larger, at 2.3%–3.0%/K. The tropics, consistently with the radiative responses shown in Figure 1a, are the dominant contributor to the spread in global mean HS. In fact, the global and tropical mean HS values in Figure 4a correlate at $r = 0.87$, compared with a mere $r = 0.20$ for global and extratropical HS (not shown). In Section 3.1, we showed that the cloud radiative response to surface warming globally reduces atmospheric radiative cooling in all assessed models (Figure 1a). By Equation 1 this is expected to weaken the release of latent heat into the atmosphere, suggesting that HS would be higher if not for cloud radiative responses. Computing HS based on all terms in Equation 1 that balance latent heating supports this. As is shown in Figure S2 in Supporting Information S1, the percent change in the sum of all balancing terms closely matches the actual HS, while omitting the cloud radiative response results in a +0.6%/K ensemble mean bias in predicted HS.

Furthermore, we now link the intermodel spread in cloud radiative response to intermodel spread in HS. In Section 3.1, we showed that clouds cause the majority of AMIP6 spread in the atmosphere's radiative response to warming (Figure 1). Precipitation and ATM radiative responses are anti-correlated at $r = -0.88$ both globally and in the tropics (Figures S3a and S3b in Supporting Information S1), while the global and tropical correlations between precipitation and ATM cloud radiative responses are $r = -0.45$ and -0.56, respectively (Figures S3c and S3d in Supporting Information S1). The latter two values are surprisingly moderate considering that the spread in global mean ATM cloud radiative response is so large it is nearly double the spread in the latent heat response. There are two reasons for why cloud radiative responses do not have a clearer influence on HS: (a) clear-sky responses are also important, correlating globally and tropically to precipitation change at $r = -0.64$ and -0.58 (Figures S3e and S3f in Supporting Information S1), and (b) interactions among cloud and clear-sky responses, which we will examine below, partly cancel the cloud radiative impact.

3.4. Verifying Cloud Radiative Impacts on Hydrological Sensitivity With Cloud Locking

We now verify that cloud radiative effects weaken hydrological sensitivity. Cloud locking allows us to isolate the impacts of cloud radiative effect changes, using simulations with CREs prescribed to values reflecting a different climate state than the underlying surface (see Section 2.3). In Figure 4b, we show the components of the global mean energetic response to surface warming in the ICON cloud locking experiment. It is apparent that cloud responses to warming do indeed weaken the precipitation change per degree of warming, reducing hydrological sensitivity by 14% globally compared to the warming response without the cloud changes (compare the circular and triangular marker for "LΔP"). Making the same comparison over the tropics instead of globally (Figure S4 in Supporting Information S1), we find the HS reduction to be 19%. As shown in the panel i of Figure 4c, the change in cloud radiative effects due to cloud responses is dominated by a shift toward enhanced radiative heating in high clouds, matching the above-described rising high cloud altitude mechanism. This weakens HS, which is primarily driven by clear-sky radiative cooling (panel iv) from temperature and humidity responses. Although we have cloud locking results from only one model, the AMIP6 models shown in Figure 2 have a similar cloud radiative response to the equivalent quantity in ICON, which is the total change in cloud radiative effects due to both cloud and clear-sky responses (panels i and iii of Figure 4c, respectively). Likewise, the hydrological sensitivity in ICON is similar to that in AMIP6, albeit slightly lower in the tropics (see Figure 4a).

With cloud locking, we can also examine in detail why cloud radiative responses to warming do not cause a 1-to-1 change in latent heat, resulting in a weaker impact on HS than expected. Critically, the latent heat from this precipitation response (LΔP) is half the magnitude of the cloud radiative response globally (compare square for "ΔCRE" to that for "LΔP" in Figure 4b), and slightly less in the tropics (Figure S4 in Supporting Information S1). This mirrors that the AMIP6 spread in latent heat response is roughly half the spread in the cloud radiative response (Figures S3c and S3d in Supporting Information S1). We find that the reduction stems from how cloud radiative responses to warming alter atmospheric temperatures and humidity (shown in Figure S5 in Supporting Information S1), and hence the clear-sky fluxes these state variables control. Most notably, because rising high clouds undergo radiative heating, the upper troposphere undergoes enhanced warming. By Stefan-Boltzmann's law this increases net emission to space, driving the upper tropospheric radiative cooling in panel ii of Figure 4c. This partly cancels the pure cloud radiative response (panel i), reducing its influence on HS. As the change in cloud radiative effects due to clear-sky responses (panel iii) is independent of cloud physical responses to warming, we discuss this separately in Text S1 in Supporting Information S1.

4. Conclusion

The key finding of our study is that high cloud radiative responses to surface warming weaken Earth's hydrological sensitivity and account for much of the AMIP6 intermodel spread in the atmosphere's energetic response to warming. The clearest mechanism behind the weakening of HS consists of high clouds enhancing radiative heating as they rise in altitude. This link between high cloud altitude and precipitation makes physical sense: much of the precipitation over tropical convective regions initiates in high clouds (Aggarwal et al., 2016), while increased radiative heating will promote evaporation in the upper atmosphere at the expense of condensation and precipitation. This finding furthers the Haslehner et al. (2024) result that high cloud CRH inhibits precipitation formation in the present-day troposphere.

There are a few caveats worth noting regarding our methods. While we have generally treated cloud responses to surface warming as a driver of atmospheric radiative and hydrological changes, this need not always be the case. For instance, reduced high cloud amount may be a result, rather than cause, of increased precipitation. We are also well aware of simplifications resulting from our use of AMIP warming experiments. In particular, we do not account for recognized influences on HS from the CO_2 direct effect (Pendergrass & Hartmann, 2014) and non-uniform SST changes (S. Zhang, Jin, & Ottaviani, 2023). One more caveat is that by focusing on HS, which is normalized by surface temperature change, we did not factor in how cloud radiative responses influence precipitation by altering the surface temperature change that develops.

Our findings offer clues for future attempts to constrain HS with climate models. First, our results suggest that past attempts to constrain HS without accounting for high cloud phenomena are insufficient. Furthermore, we have shown that high cloud impacts on HS involve multiple, potentially co-varying, mechanisms. Given such complexity, it seems plausible that no strong constraint on HS would consist of a simple constraint on cloud processes. Still, improved estimates of HS may follow efforts to reliably simulate the radiative, microphysical,

and dynamical processes that govern precipitation change. Part of the intermodel HS spread likely results from climatological differences in high clouds (c.f. Po-Chedley et al., 2019), so better simulating observed present-day cloud properties may be one route to constraining HS.

Data Availability Statement

CMIP6 model output is publicly available online at https://pcmdi.llnl.gov/CMIP6/. We have placed the examined ICON cloud locking model output on a Zenodo archive (Voigt, Van de Koot, & McGraw, 2024).

Acknowledgments
LMP acknowledges funding from the US National Science Foundation to Columbia University (award 2335762). BG and AV acknowledge funding from the EU's Horizon 2020 research and innovation programme (Marie Sklodowska-Curie grant 101025473). EV acknowledges funding from the UK Natural Environmental Research Council, Doctoral Training Partnership in Environmental Research (Grant NE/S007474/1).

References

Aggarwal, P. K., Romatschke, U., Araguas-Araguas, L., Belachew, D., Longstaffe, F. J., Berg, P., et al. (2016). Proportions of convective and stratiform precipitation revealed in water isotope ratios. *Nature Geoscience*, *9*(8), 624–629. https://doi.org/10.1038/ngeo2739

Bony, S., Stevens, B., Coppin, D., Becker, T., Reed, K. A., Voigt, A., & Medeiros, B. (2016). Thermodynamic control of anvil cloud amount. *Proceedings of the National Academy of Sciences of the United States of America*, *113*(32), 8927–8932. https://doi.org/10.1073/pnas.1601472113

Eyring, V., Bony, S., Meehl, G. A., Senior, C. A., Stevens, B., Stouffer, R. J., & Taylor, K. E. (2016). Overview of the coupled model Intercomparison Project Phase 6 (CMIP6) experimental design and organization. *Geoscientific Model Development*, *9*(5), 1937–1958. https://doi.org/10.5194/gmd-9-1937-2016

Giorgetta, M. A., Brokopf, R., Crueger, T., Esch, M., Fiedler, S., Helmert, J., et al. (2018). ICON-A, the atmosphere component of the ICON earth system model: I. Model description. *Journal of Advances in Modeling Earth Systems*, *10*(7), 1613–1637. https://doi.org/10.1029/2017ms001242

Hartmann, D. L., & Larson, K. (2002). An important constraint on tropical cloud-climate feedback. *Geophysical Research Letters*, *29*(20), 1951. https://doi.org/10.1029/2002gl015835

Haslehner, K., Gasparini, B., & Voigt, A. (2024). Radiative heating of high-level clouds and its impacts on climate. *Journal of Geophysical Research: Atmospheres*, *129*(12), e2024JD040850. https://doi.org/10.1029/2024jd040850

Hendrickson, J. M., Terai, C. R., Pritchard, M. S., & Caldwell, P. M. (2021). Lower tropospheric processes: A control on the global mean precipitation rate. *Geophysical Research Letters*, *48*(6), e2020GL091169. https://doi.org/10.1029/2020gl091169

Huber, M. (2024). *Atmospheric and surface pathways of the cloud-radiative impact on the circulation response to warming*. Masters thesis. University of Vienna. Retrieved from https://utheses.univie.ac.at/detail/63548/

Jeevanjee, N., & Romps, D. M. (2018). Mean precipitation change from a deepening troposphere. *Proceedings of the National Academy of Sciences of the United States of America*, *115*(45), 11465–11470. https://doi.org/10.1073/pnas.1720683115

Liu, J., Yang, J., Ding, F., Chen, G., & Hu, Y. (2024). Hydrologic cycle weakening in hothouse climates. *Science Advances*, *10*(17), eado2515. https://doi.org/10.1126/sciadv.ado2515

Muller, C. J., & O'Gorman, P. A. (2011). An energetic perspective on the regional response of precipitation to climate change. *Nature Climate Change*, *1*(5), 266–271. https://doi.org/10.1038/nclimate1169

O'Gorman, P. A., Allan, R. P., Byrne, M. P., & Previdi, M. (2012). Energetic constraints on precipitation under climate change. *Surveys in Geophysics*, *33*(3–4), 585–608. https://doi.org/10.1007/s10712-011-9159-6

Pendergrass, A. G. (2020). The global-mean precipitation response to CO_2-induced warming in CMIP6 models. *Geophysical Research Letters*, *47*(17), e2020GL089964. https://doi.org/10.1029/2020gl089964

Pendergrass, A. G., & Hartmann, D. L. (2014). The atmospheric energy constraint on global-mean precipitation change. *Journal of Climate*, *27*(2), 757–768. https://doi.org/10.1175/jcli-d-13-00163.1

Po-Chedley, S., Zelinka, M. D., Jeevanjee, N., Thorsen, T. J., & Santer, B. D. (2019). Climatology explains intermodel spread in tropical upper tropospheric cloud and relative humidity response to greenhouse warming. *Geophysical Research Letters*, *46*(22), 13399–13409. https://doi.org/10.1029/2019gl084786

Previdi, M. (2010). Radiative feedbacks on global precipitation. *Environmental Research Letters*, *5*(2), 025211. https://doi.org/10.1088/1748-9326/5/2/025211

Sherwood, S. C., Webb, M. J., Annan, J. D., Armour, K. C., Forster, P. M., Hargreaves, J. C., et al. (2020). An assessment of Earth's climate sensitivity using multiple lines of evidence. *Reviews of Geophysics*, *58*(4), e2019RG000678. https://doi.org/10.1029/2019rg000678

Soden, B. J., Held, I. M., Colman, R., Shell, K. M., Kiehl, J. T., & Shields, C. A. (2008). Quantifying climate feedbacks using radiative kernels. *Journal of Climate*, *21*(14), 3504–3520. https://doi.org/10.1175/2007jcli2110.1

Voigt, A., North, S., Gasparini, B., & Ham, S. H. (2024). Atmospheric cloud-radiative heating in CMIP6 and observations and its response to surface warming. *Atmospheric Chemistry and Physics*, *24*(17), 9749–9775. https://doi.org/10.5194/acp-24-9749-2024

Voigt, A., & Shaw, T. A. (2015). Circulation response to warming shaped by radiative changes of clouds and water vapour. *Nature Geoscience*, *8*(2), 102–106. https://doi.org/10.1038/ngeo2345

Voigt, A., Van de Koot, E. K., & McGraw, Z. (2024). Output from ICON v2.6.2.2 cloud locking simulations: 3D radiative fluxes and additional atmospheric variables [Dataset]. *Zenodo*. https://doi.org/10.5281/zenodo.14278725

Watanabe, M., Kamae, Y., Shiogama, H., DeAngelis, A. M., & Suzuki, K. (2018). Low clouds link equilibrium climate sensitivity to hydrological sensitivity. *Nature Climate Change*, *8*(10), 901–906. https://doi.org/10.1038/s41558-018-0272-0

Yoshimori, M., Lambert, F. H., Webb, M. J., & Andrews, T. (2020). Fixed anvil temperature feedback: Positive, zero, or negative? *Journal of Climate*, *33*(7), 2719–2739. https://doi.org/10.1175/jcli-d-19-0108.1

Zelinka, M. D., Klein, S. A., & Hartmann, D. L. (2012a). Computing and partitioning cloud feedbacks using cloud property histograms. Part I: Cloud radiative kernels. *Journal of Climate*, *25*(11), 3715–3735. https://doi.org/10.1175/jcli-d-11-00248.1

Zelinka, M. D., Klein, S. A., & Hartmann, D. L. (2012b). Computing and partitioning cloud feedbacks using cloud property histograms. Part II: Attribution to changes in cloud amount, altitude, and optical depth. *Journal of Climate*, *25*(11), 3736–3754. https://doi.org/10.1175/jcli-d-11-00249.1

Zelinka, M. D., Myers, T. A., McCoy, D. T., Po-Chedley, S., Caldwell, P. M., Ceppi, P., et al. (2020). Causes of higher climate sensitivity in CMIP6 models. *Geophysical Research Letters*, *47*(1), e2019GL085782. https://doi.org/10.1029/2019gl085782

Zelinka, M. D., Zhou, C., & Klein, S. A. (2016). Insights from a refined decomposition of cloud feedbacks. *Geophysical Research Letters*, *43*(17), 9259–9269. https://doi.org/10.1002/2016gl069917

Zhang, S., Stier, P., Dagan, G., Zhou, C., & Wang, M. (2023). Sea surface warming patterns drive hydrological sensitivity uncertainties. *Nature Climate Change*, *13*(6), 545–553. https://doi.org/10.1038/s41558-023-01678-5

Zhang, Y., Jin, Z., & Ottaviani, M. (2023). Comparison of clouds and cloud feedback between AMIP5 and AMIP6. *Atmosphere*, *14*(6), 978. https://doi.org/10.3390/atmos14060978

Zhang, Y., Jin, Z., & Sikand, M. (2021). The top-of-atmosphere, surface and atmospheric cloud radiative kernels based on ISCCP-H datasets: Method and evaluation. *Journal of Geophysical Research: Atmospheres*, *126*(24), e2021JD035053. https://doi.org/10.1029/2021jd035053

Zhou, W., Leung, L. R., Siler, N., & Lu, J. (2023). Future precipitation increase constrained by climatological pattern of cloud effect. *Nature Communications*, *14*(1), 6363. https://doi.org/10.1038/s41467-023-42181-x